

ZirTiDiS: an implicit finite difference code for the calculation of apparent Zr-in-Titanite (ZiT) temperatures

Simon Schorn* & Evangelos Moulas

Institute of Geosciences, Johannes-Gutenberg University Mainz, Germany

*schorsim@uni-mainz.at

Here we describe the application of ZirTiDiS (**Z**irconium in **T**itanite **D**iffusion **S**oftware), a set of MATLAB routines designed to calculate apparent Zirconium-in-Titanite temperatures in function of a sample's pressure–temperature–composition evolution using the thermobarometer of Hayden et al. (2008). Using Hayden et al.'s equation, the equilibrium Zr concentration in titanite (sphene) is calculated for a custom pressure–temperature–time path by specifying start- and end conditions, a cooling rate and the activities of TiO_2 and SiO_2 required for the thermobarometer. Alternatively, activities can be calculated using bulk-composition-specific phase diagrams (pseudosections) and lookup-tables containing chemical potential data from which the activities of TiO_2 and SiO_2 are calculated. The Zr concentration and the respective effective Zr-in-titanite (ZiT) temperature is calculated for spherical grains considering thermally activated diffusion, using experimentally derived diffusion coefficients for Zr in titanite (Cherniak, 2006). We then present a worked example and benchmarks detailing the main features of ZirTiDiS.

The following routines must be located in the same directory:

- [ZirTiDiS_fun.m](#): main function
- [ZirTiDiS_exe.m](#): calculate cooling histories
- [ZirTiDiS_CR_exe.m](#): calculate apparent ZiT Temperatures vs. cooling rates
- [data.dat](#): chemical potential database

and the main code is executed by typing [ZirTiDiS_exe](#) or [ZirTiDiS_CR_exe](#) in the MATLAB command window.

The code is written in a general way to allow for a transparent presentation of the results and is provided free of charge¹. All software and documentation presented here is intended for research and didactic purpose and comes without warranty.

Current Version: 1.0 (13.05.2024) – 10.5281/zenodo.11184086

In case of questions or remarks please send an email to simschor@uni-mainz.de

¹ Creative Commons Attribution 4.0 International

CONTENTS

GOVERNING EQUATIONS	3
The Zr-in-titanite thermobarometer	3
Diffusion in a sphere.....	3
Numerical solution of the diffusion equation.....	3
PRESSURE–TEMPERATURE–ACTIVITY PATHS & EXAMPLES.....	4
User-specified activities	4
Activities from pseudosections	7
Cooling rates	7
CODE TESTING	8
Numerical resolution and convergence.....	8
Analytical benchmark.....	8
REFERENCES.....	10
APPENDIX.....	10
Pseudosection calculation.....	10
Calculating activities from chemical potentials.....	11
REFERENCES (Appendix)	11

GOVERNING EQUATIONS

The Zr-in-titanite thermobarometer

Hayden et al. (2008) experimentally calibrated the pressure–temperature–activity relationship for the Zr concentration in titanite. Their thermobarometer is sensitive to the activities of TiO₂ and SiO₂, which can be either specified by the user or calculated for a chosen bulk rock composition.

The equilibrium Zr concentration in titanite as a function of temperature, pressure and activities is given by:

$$\log(Zr_{ppm}^{titanite}) = 10.52 - \frac{7708}{T(K)} - 960 \frac{P(\text{GPa})}{T(K)} - \log(a_{\text{TiO}_2}) - \log(a_{\text{SiO}_2}) \quad (1)$$

(Hayden et al. 2008). Rearranged for temperature, equation (1) becomes:

$$T(^{\circ}\text{C}) = \frac{7708 + 960P(\text{GPa})}{10.52 - \log(a_{\text{TiO}_2}) - \log(a_{\text{SiO}_2}) - \log(Zr_{ppm}^{titanite})} - 273 \quad (2)$$

The thermobarometer was calibrated using Zr contents in titanite crystals synthesized in the presence of zircon, quartz and rutile at 1–2.4 GPa and 800–1000°C in a piston cylinder apparatus. The estimated uncertainty is ±20°C within the range of 600–1000°C (Hayden et al. 2008).

Diffusion in a sphere

For one-dimensional diffusion in a spherical geometry, the change in concentration with respect to time is proportional to the radial derivative of the concentration gradient:

$$\frac{\partial C}{\partial t} = \frac{D(T)}{r^2} \frac{\partial}{\partial r} \left(r^2 \frac{\partial C}{\partial r} \right) \quad (3)$$

Where t is time, r is the radial direction, $C(r,t)$ is the concentration and $D(T)$ is temperature-dependent diffusivity of the Arrhenius-type:

$$D(T) = D_0 \exp\left(-\frac{Q}{RT}\right) \quad (4)$$

With D_0 ($5.33 \cdot 10^{-7}$ m²/sec) being the diffusivity at infinite temperature (pre-exponent factor) and Q ($325 \cdot 10^3$ J/mol) the activation energy that are experimentally determined for titanite under anhydrous, pO₂-buffered conditions (Cherniak, 2006). T is the absolute temperature and R is the gas constant (8.314 J/mol/K). No pressure dependence on the diffusivity is reported. These are currently the only available estimates for diffusivity in titanite; however, the code can be easily updated if required.

Numerical solution of the diffusion equation

The diffusion equation (3) is solved using an implicit finite difference scheme yielding

$$C_i^n [1 + S(r_{CR}^2 + r_{CL}^2)] - SC_{i+1}^n r_{CR}^2 - SC_{i-1}^n r_{CL}^2 = C_i^o \quad (5)$$

where r_{CR} and r_{CL} is the midpoint to the right and left of the evaluated grid node i , respectively.

While

$$S = \frac{D(T)\Delta t}{r^2\Delta r^2} \quad (6)$$

combines thermally activated diffusivity (equation 4) with the spatial- (Δr) and temporal discretization (Δt). The initial condition is given by the Zr concentration calculated for the starting temperature and allocated to the entire grain (i.e., homogenous concentration). The concentration is calculated for a spherical half-grain and symmetry is achieved via a zero-flux (Neumann) boundary condition at the grain center. The (Dirichlet) boundary condition at the grain rim is updated at each time step and given by the Zr concentration at the new pressure–temperature–activity conditions calculated for the user-specified cooling rate, decompression rate and/or changing activities using equation (1).

PRESSURE–TEMPERATURE–ACTIVITY PATHS & EXAMPLES

User-specified activities

Table 1 shows the main user input required to execute the program:

Table 1 – Code snipped from *ZirTiDiS_exe.m* showing the main user input data.

```
clear,clc,close all
%-----
% ZirTiDiS - Zirconium-in-Titanite Diffusion Software
% S. Schorn & E. Moulas - Mainz, 18.05.2024
%for more details see Zenodo documentation
%doi: 10.5281/zenodo.11184086
%#+-----+
%CALCULATE COOLING HISTORIES
%#+-----+
%-----
%IMPLICIT SOLVER
%-----
plot_now      = 1;           %[0,1] - 1 for plotting on the fly
lookupable   = 0;           %[0,1] - 1 to load precompiled data
safe_data    = 0;           %[0,1] - 1 to safe data
%#+-----+
%define your system here
grsz         = 50;           %grain radius          [µm]
Tin          = 800;          %initial temperature [°C]
Tfin         = 600;          %final temperature  [°C]
cool_r       = 20;           %cooling rate       [°C/myr]
tstep        = 1e10;         %time step (~1e10 - 1e11)
C2K          = 273;          %convert °C to K
myr2sec      = 60*60*24*365*1e6; %million year [s]
%if isobaric: set Pin = Pfin
Pin          = 1.0;          %initial pressure [GPa]
Pfin         = 0.4;          %final pressure  [GPa]
%set activities - used if lookup tabel == 0
aTi_in       = 1.0;          %starting activity TiO2
aTi_fin      = 1.0;          %ending activity TiO2
aSi_in       = 1.0;          %starting activity SiO2
aSi_fin      = 1.0;          %ending activity SiO2
%#+-----+
```

A typical cooling history output using `ZirTiDiS_exe.m` for fixed activities (`lookuptable = 0`) is presented in Figure 1. The program calculates the initial Zr concentration of ~276.5 ppm for the specified starting conditions which is allocated to the entire grain. Due to the imposed cooling rate, the temperature decreases for each time step and the associated Zr concentration is calculated and allocated to the grain rim. This results in a Zr concentration gradient which drives diffusion from the core towards the rim to equalize the concentration. At high temperature diffusion is efficient and the Zr concentration at the center approximates the equilibrium concentration imposed at the rim. Therefore, the recorded ZiT core temperature remains close to the actual temperature during cooling – the red line ('T in titanite') does not significantly depart from the blue line ('real T'). However, with decreasing temperature the diffusive equilibration between core and rim becomes increasingly ineffective, resulting in an incremental departure of the ZiT core temperature from the actual one. The final Zr concentration throughout the grain describes a characteristic bell-shaped profile, with a maximum at the core (~136.7 ppm) and minimum at the rim (~17.8 ppm), corresponding to an apparent ZiT temperature of ~692°C and ~600°C, respectively (Fig. 1).

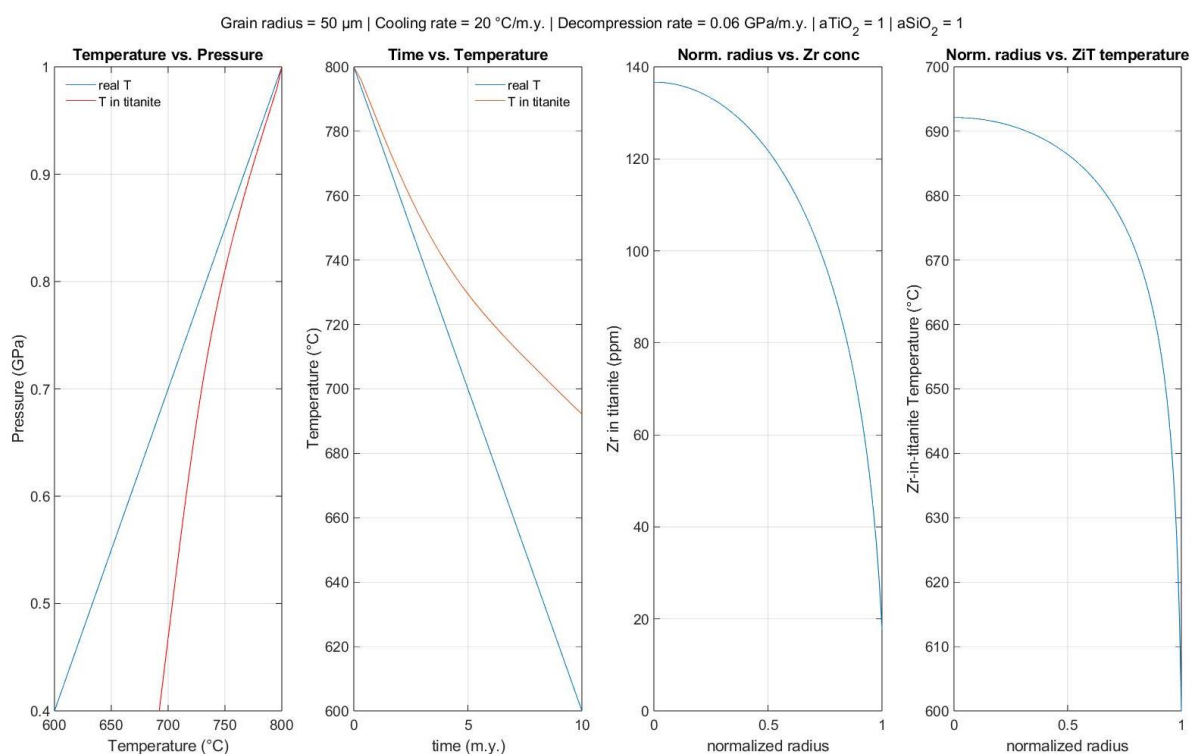


Figure 1 – Example calculation for a_{TiO_2} and a_{SiO_2} of unity. The red line is the calculated apparent ZiT core temperature.

Some key results are prompted in the command window:

Table 2 – Command window prompt for previous calculation.

```

Command Window
Elapsed time is 4.824951 seconds.
Initial Zr concentration in the grain is 276.5125 ppm.
Final rim Zr concentration is 17.818 ppm.
Final core Zr concentration is 136.6765 ppm.
Zr-in-titanite temperature at the core is 692.1365  $^{\circ}\text{C}$ .
fx >>

```

The equilibrium Zr concentration in titanite calculated using equation (1) as a function of pressure and temperature for activities equal to unity is shown in Figure 2 (left), while the effect of variable activities is displayed in the panel to the right. Similar concentrations are used as boundary condition for the grain rim.

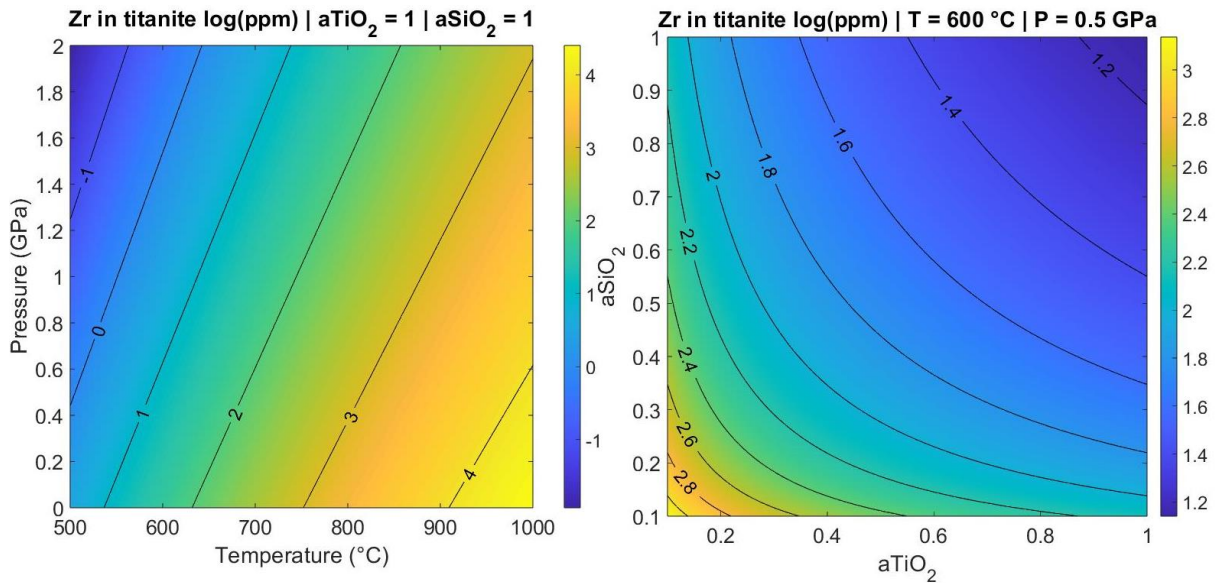


Figure 2 – Pressure–Temperature space contoured for equilibrium Zr concentration in titanite and concentration at a fixed P–T point in function of aTiO₂ and aSiO₂ (log₁₀ units ppm).

It is pointed out that the choice of activities affects the absolute Zr concentration (Fig. 3, left), but not the apparent ZiT temperature (Fig. 3, right). However, this is only true if the activities are kept constant throughout the calculation run (cf. yellow line).

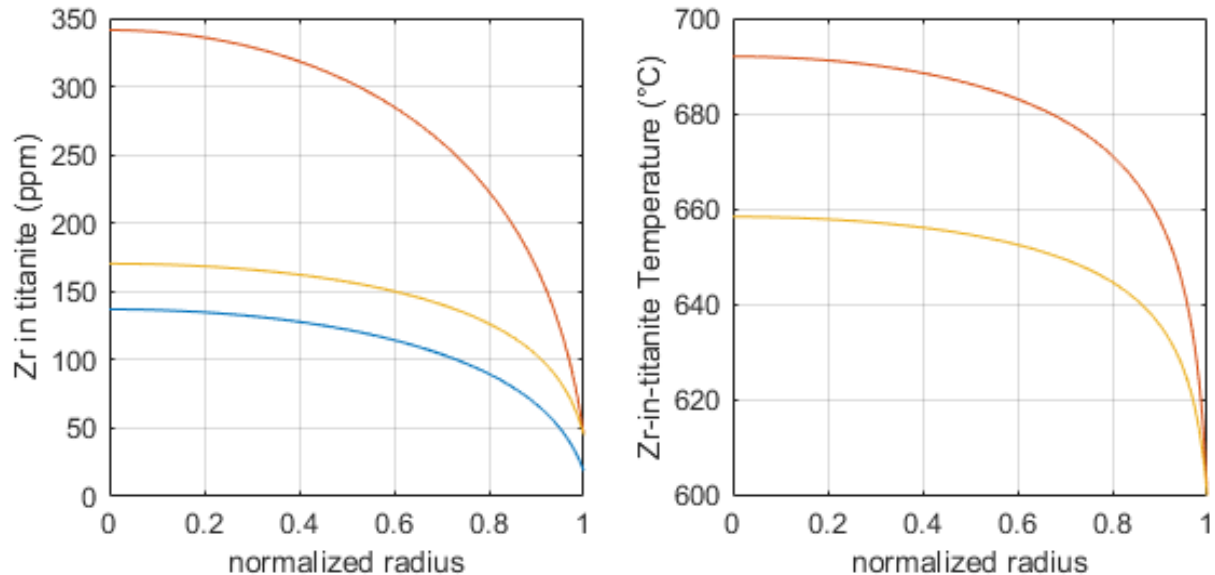


Figure 3 – Calculation showing the effect of activities. Blue: aTiO₂ = aSiO₂ = 1.0. Red: aTiO₂ = 0.8, aSiO₂ = 0.5. Note that the blue and red line overlap in the right panel. Yellow: starting conditions are the same as for the blue line, final conditions are those of the red line. Other parameters are identical to those in Figure 1.

Activities from pseudosections

As alternative to user-specified activities, a lookup table ('data.dat' in the current example) containing precomputed chemical potential data can be used (`lookuptable = 1`) to calculate activities from bulk-composition specific phase diagrams (aka pseudosections). In this example, we base our calculations on a MOR basalt (SM89 104–16; Sun & McDonough 1989), carried out using the Perple_X software bundle (Connolly, 2005, 2009). Details on the construction of the phase diagram and activity calculation can be found in the Appendix. Figure 4 shows the activities for TiO_2 and SiO_2 and the respective Zr concentration in titanite.

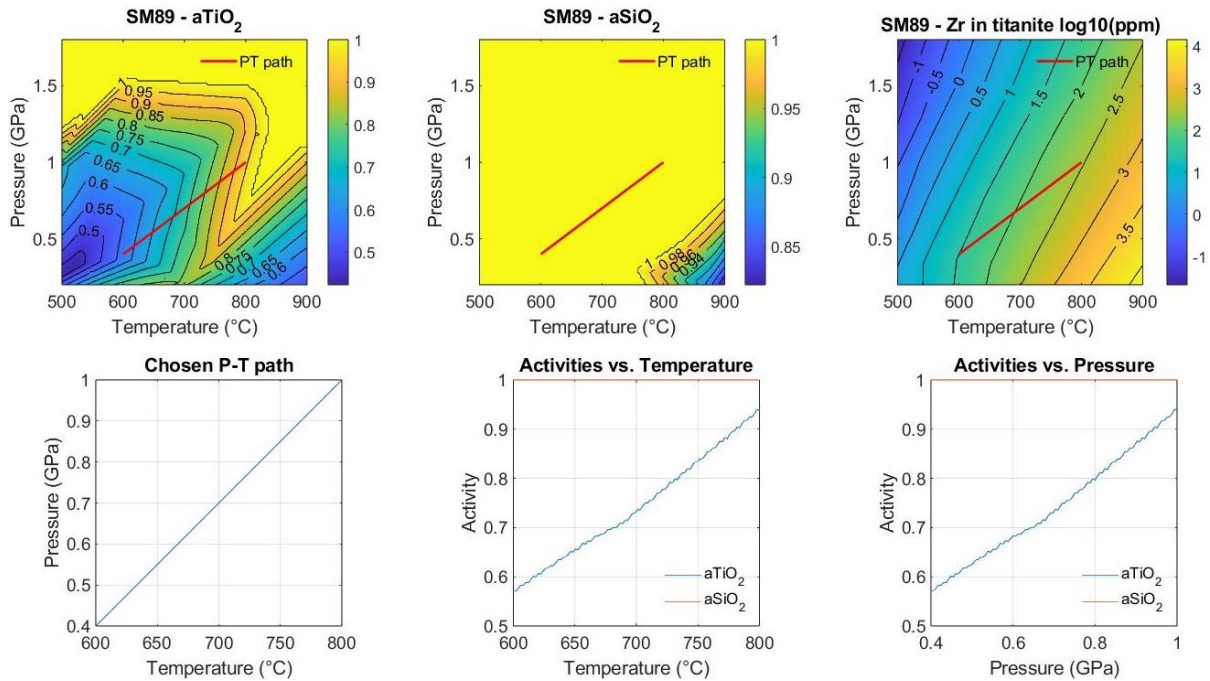


Figure 4 – Activities and equilibrium Zr concentration for the SM89 MORB.

Cooling rates

ZirTiDiS can be executed repeatedly for increasing cooling rates to calculate apparent temperatures depending on grain size and initial temperature (Fig. 5). This is done in the routine `ZirTiDiS_CR_exe.m`. It should be noted that this type of calculation is independent of the choice of pressure and activities, so long as the values are kept constant during cooling.

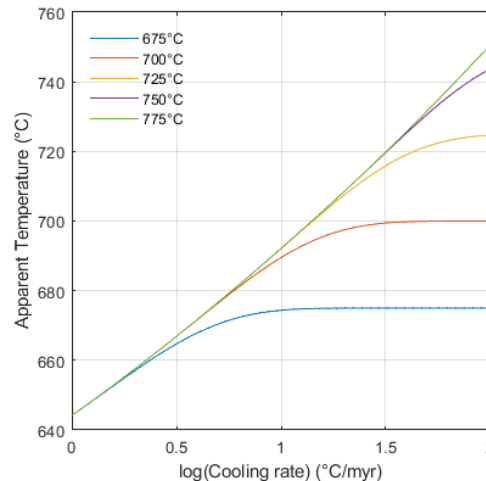


Figure 5 – ZrTi core temperature as function of cooling rate & initial temperature (colored lines). Grain size = 25 μm .

CODE TESTING

Numerical resolution and convergence

In ZirTiDiS, the diffusion equation is solved using an implicit finite difference scheme; as such, it is unconditionally stable for any choice of time step `tstep` (which is set by the user). Depending on the type of calculation, it may be useful to increase `tstep` to speed up the calculations. In this case it is recommended to perform a convergence test (e.g., Fig. 6) to ensure that the calculated ZiT temperatures approximate a unique value (~740°C in this example). In the current example and depending on the machine used, a calculation takes ~4 seconds for `tstep = 1e10`. Such small time steps are only required to produce a smooth cooling history (e.g., red line on Fig. 1), but can be increased to ~1e11 without significantly affecting the calculated final ZiT core temperature (Fig. 6, left). With this `tstep` a typical calculation takes ~0.5 seconds (Fig. 6, right).

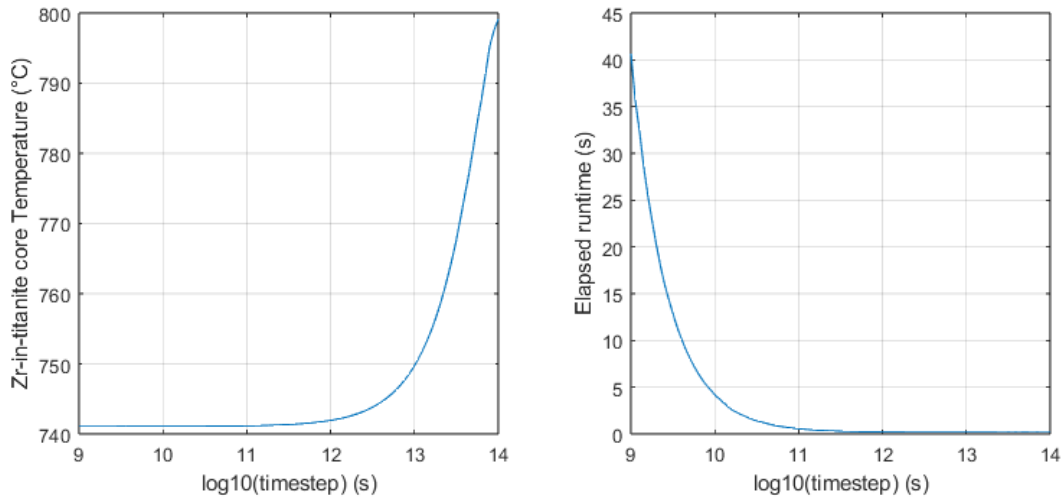


Figure 6 – Left: ZiT core Temperature (°C) vs. timestep (\log_{10} units seconds). Right: Runtime (s) vs. timestep. Pressure is 1 GPa and activities are unity. Other parameters are identical to those in Fig. 1.

Analytical benchmark

The numerical solution is benchmarked against an analytical expression (Crank, 1979, eq. 6.18) for time-dependent diffusivity and a linear cooling path (i.e., a constant cooling rate) as shown in Figure 6a. According to eq. (4), the effective diffusivity exponentially decays with decreasing temperature (Fig. 6b). It was shown that by defining a new ‘compressed time’ variable τ (after Lasaga, 1983; Fig. 6c, d), the problem involving temperature-dependent diffusivity (\tilde{D}) effectively reduces to one with constant diffusivity (i.e., isothermal). This is graphically highlighted by the colored areas under the curves in figures 6c and d being equivalent. The analytical solution is given by:

$$C(r, \tau) = -\frac{2LC_0}{\pi r} \sum_{n=1}^{n=\infty} \frac{(-1)^n}{n} \exp(-n^2 X) \sin\left(\frac{n\pi r}{L}\right)$$

$$X = \frac{\pi^2}{L^2} \tau D_{max}$$

$$\tau = \int_0^t \frac{\tilde{D}(t')}{D_{max}} dt'$$

$$\tilde{D} = D(T(t))$$

where C is the concentration at a given radial coordinate r and time t , C_0 is the starting concentration throughout the grain, D_{max} is the diffusivity at maximum temperature and L is the total grain radius. This solution applies for a constant (Dirichlet) boundary condition of 0 concentration at the grain rim where $r = L$ (Fig. 6e). The infinite sum is truncated after 30 terms, after which the residuals become negligible ($\sim 10^{-20}$; Fig. 6f).

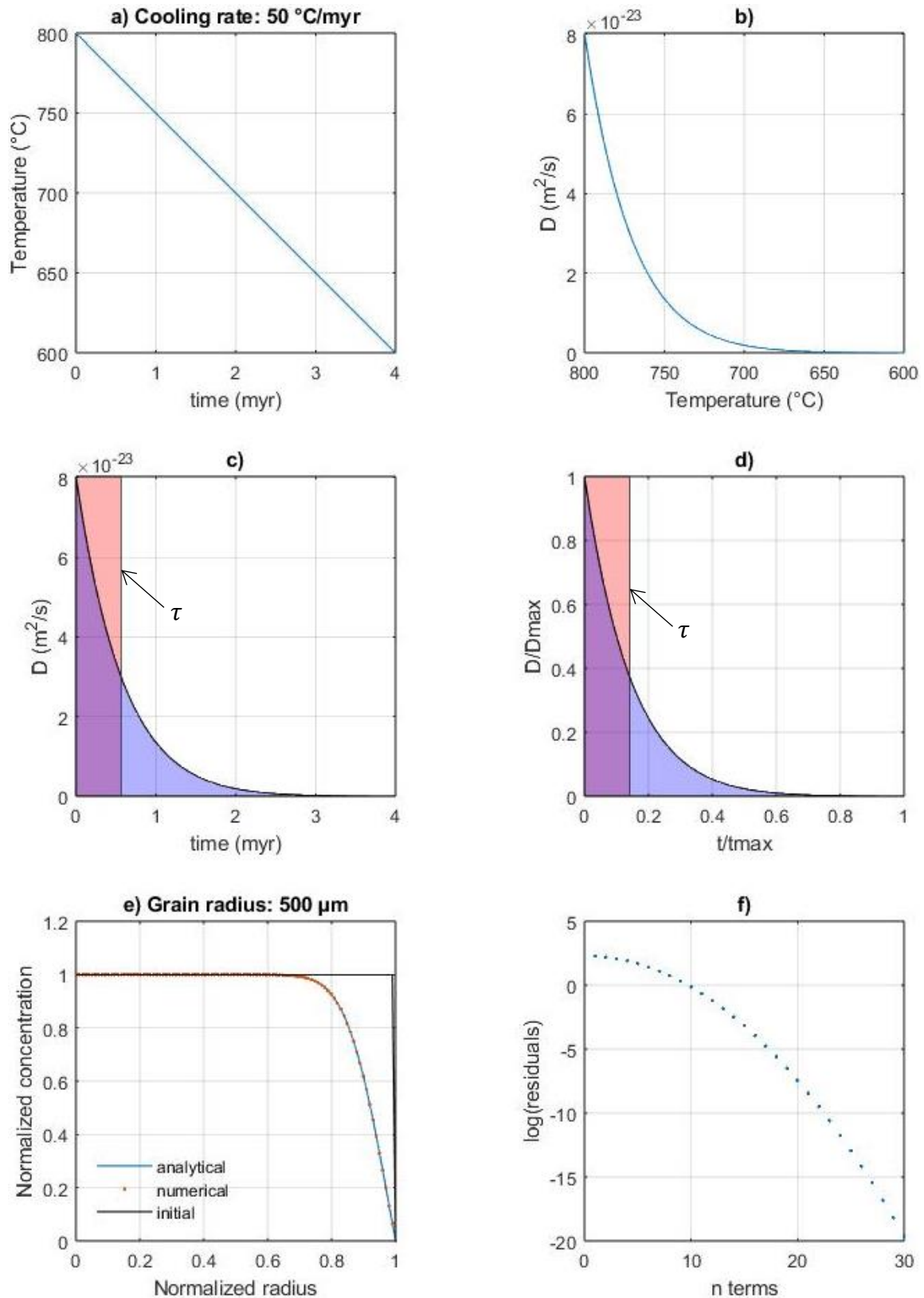


Figure 7 – Numerical vs. analytical solution for time-dependent diffusivity.

REFERENCES

- Cherniak, D. J. (2006). Zr diffusion in titanite. *Contributions to Mineralogy and Petrology*, 152, 639–647.
- Connolly, J., 2009. The geodynamic equation of state: what and how. *Geochemistry, geophysics, geosystems*, 10(10).
- Connolly, J. A., 2005. Computation of phase equilibria by linear programming: a tool for geodynamic modeling and its application to subduction zone decarbonation. *Earth and Planetary Science Letters*, 236(1-2), 524–541.
- Crank, J. (1979). *The mathematics of diffusion*. Oxford university press.
- Hayden, L. A., Watson, E. B., & Wark, D. A. (2008). A thermobarometer for sphene (titanite). *Contributions to Mineralogy and Petrology*, 155, 529–540.
- Lasaga, A. C. (1983). Geospeedometry: an extension of geothermometry. In *Kinetics and equilibrium in mineral reactions* (pp. 81-114). New York, NY: Springer New York.
- Sun, S. S., & McDonough, W. F. (1989). Chemical and isotopic systematics of oceanic basalts: implications for mantle composition and processes. *Geological Society, London, Special Publications*, 42(1), 313–345.

APPENDIX

Pseudosection calculation

Pseudosection calculations were performed using *Perple_X* v.7.0.11 (Connolly, 2005, 2009) and the thermodynamic dataset *hp62ver.dat* (Holland & Powell, 2011). The employed activity–composition relationships are *Fsp(C1)* for feldspars (Holland & Powell, 2003), *cAmph(G)*, *Augite(G)* and *melt(G)* for clinoamphibole, augitic clinopyroxene and mafic melt, respectively (Green et al., 2016), *Gt(W)*, *Chl(W)*, *Bi(W)*, *Mica(W)*, *Opx(W)* and *Ilm(DS6)* for garnet, chlorite, biotite, white mica, orthopyroxene and ilmenite, respectively (White et al., 2014), *Ep(HP11)* for epidote (Holland & Powell, 2011) and *O(HP)* for olivine (Holland & Powell, 1998). The whole rock composition (MORB 104–16 of Sun & McDonough, 1998) is converted to the model system of $\text{Na}_2\text{O}–\text{CaO}–\text{K}_2\text{O}–\text{FeO}–\text{MgO}–\text{Al}_2\text{O}_3–\text{SiO}_2–\text{H}_2\text{O}–\text{TiO}_2–\text{O}_2$ (NCKFMASHTO) by omitting minor MnO and converting 30% of the total FeO to Fe_2O_3 (Table S1). Similarly, phase diagrams are constructed for pure TiO_2 (rutile) and SiO_2 (quartz) to calculate the reference chemical potentials (see below). Input- & output datafiles and phase diagrams can be found in the supplementary materials. For additional details on phase diagram calculations and using WERAMI visit <https://www.perplex.ethz.ch/>.

Table S1 – Whole rock bulk composition of MORB 104–16 (wt.%) used for thermodynamic modelling.

SiO ₂	TiO ₂	Al ₂ O ₃	FeO	MgO	CaO	Na ₂ O	K ₂ O	O ₂	H ₂ O	Sum
50.22	1.34	14.79	9.33	8.17	10.92	2.58	0.34	0.31	2.00	100.00

Calculating activities from chemical potentials

The chemical potential of a component i is related to the activity and the absolute temperature via the relationship

$$\mu_i = \mu_0 + RT \ln a_i \quad (\text{A1})$$

where μ_0 is the reference chemical potential at the standard state. Rearranged for activity this yields

$$a_i = \exp\left(\frac{\mu_i - \mu_0}{RT}\right) \quad (\text{A2})$$

For the calculations at hand, the chemical potentials of TiO_2 and SiO_2 can be easily computed using WERAMI from the Perple_X software bundle. In this case, μ_i is the chemical potential of component i (e.g., TiO_2) calculated for the specified bulk rock composition (MORB 104–16 here) while μ_0 relates to the chemical potential of component i in the pure reference phase (i.e., rutile). For μ_{SiO_2} this corresponds to pure quartz. The compiled datatable ('[data.dat](#)') feeds into the '[activity_data_function](#)', which calculates the activities using equation (A2). Reasonably, where the calculated mineral assemblages contain rutile and quartz, μ_i and μ_0 are equal and therefore $a_{\text{TiO}_2} = a_{\text{SiO}_2} = 1.0$ (Fig. 4).

REFERENCES (Appendix)

Green, E. C. R., White, R. W., Diener, J. F. A., Powell, R., Holland, T. J. B., & Palin, R. M. (2016). Activity–composition relations for the calculation of partial melting equilibria in metabasic rocks. *Journal of Metamorphic Geology*, 34(9), 845-869.

Holland, T.J.B., & Powell, R. (2003). Activity–composition relations for phases in petrological calculations: an asymmetric multicomponent formulation. *Contributions to Mineralogy and Petrology*, 145, 492-501.

Holland, T. J. B., & Powell, R. T. J. B. (1998). An internally consistent thermodynamic data set for phases of petrological interest. *Journal of metamorphic Geology*, 16(3), 309-343.

Holland, T. J. B., & Powell, R. (2011). An improved and extended internally consistent thermodynamic dataset for phases of petrological interest, involving a new equation of state for solids. *Journal of metamorphic Geology*, 29(3), 333-383.

White, R. W., Powell, R. O. G. E. R., Holland, T. J. B., Johnson, T. E., & Green, E. C. R. (2014). New mineral activity–composition relations for thermodynamic calculations in metapelitic systems. *Journal of Metamorphic Geology*, 32(3), 261-286.